

**Enhanced superconductivity by near-neighbor attraction in the doped extended Hubbard model**Cheng Peng <sup>1</sup>, Yao Wang,<sup>2</sup> Jiajia Wen,<sup>1</sup> Young S. Lee,<sup>1,3</sup> Thomas P. Devereaux,<sup>1,4</sup> and Hong-Chen Jiang<sup>1,\*</sup><sup>1</sup>*Stanford Institute for Materials and Energy Sciences, SLAC National Accelerator Laboratory, Menlo Park, California 94025, USA*<sup>2</sup>*Department of Physics and Astronomy, Clemson University, Clemson, South Carolina 29631, USA*<sup>3</sup>*Department of Applied Physics, Stanford University, Stanford, California 94305, USA*<sup>4</sup>*Department of Materials Science and Engineering, Stanford University, Stanford, California 94305, USA*

(Received 10 June 2022; revised 20 February 2023; accepted 3 April 2023; published 3 May 2023)

A recent experiment has unveiled an anomalously strong electron-electron attraction in the one-dimensional copper-oxide chain  $\text{Ba}_{2-x}\text{Sr}_x\text{CuO}_{3+\delta}$ . While the effect of the near-neighbor electron attraction  $V$  in the one-dimensional extended Hubbard chain has been examined recently, its effect in the Hubbard model beyond the one-dimensional chain remains unclear. Here, we report a density matrix renormalization group study of the extended Hubbard model on long four-leg cylinders on the square lattice. We find that the near-neighbor electron attraction  $V$  can notably enhance the long-distance superconducting correlations while simultaneously suppressing the charge-density-wave (CDW) correlations. Specifically, for a modestly strong electron attraction, the superconducting correlations become dominant over the CDW correlations with a Luttinger exponent  $K_{sc} \sim 1$  and strong divergent superconducting susceptibility. Our results provide a promising way to realize long-range superconductivity in the doped Hubbard model. The relevance of our numerical results to cuprate materials is also discussed.

DOI: [10.1103/PhysRevB.107.L201102](https://doi.org/10.1103/PhysRevB.107.L201102)

The origin of unconventional superconductivity is one of the greatest mysteries since the discovery of high- $T_c$  cuprates [1]. Contrary to the conventional BCS superconductors, it is widely believed that the strong electronic Coulomb repulsions in the  $3d$  orbitals play the dominant role in the  $d$ -wave pairing mechanism in cuprates. Along this line, spin fluctuations generated by the doped antiferromagnetic state may provide the pairing glue [2–5]. Based on the minimal model describing the correlations effect—the single-band Hubbard model [6–10]—this pairing mechanism has been proposed based on perturbation theory and instabilities on small clusters [11,12]. However, the ultimate verification requires the exact proof of long-range-order  $d$ -wave superconductivity in the thermodynamic limit.

To address these questions, advanced numerical simulations have been applied to the Hubbard model and its low-energy analog—the  $t$ - $J$  model—in the past few years [9,10]. Many unusual phases in cuprates, such as a striped phase [13–16] and a strange metal phase [17–19], have been identified recently by unbiased and exact methods on clusters such as density matrix renormalization group (DMRG) and determinantal quantum Monte Carlo (DQMC). However, the search for a  $d$ -wave superconducting (SC) phase has not been quite as successful [20]. Quasi-long-range SC order has been found in the Hubbard and  $t$ - $J$  models on four-leg square lattice cylinders [21–29], which may be tuned by the band structure and in the striped Hubbard model [30]. However, when a similar study was extended to the wider six- and eight-leg  $t$ - $J$  cylinders on the square lattice, which is closer to two

dimensions, superconductivity is found to disappear in the hole-doped side [26–28]. Therefore, the original Hubbard and  $t$ - $J$  models themselves might be insufficient to resolve the high- $T_c$  puzzle.

Meanwhile, experimental efforts have been devoted to the search for new insights. In a very recent photoemission experiment, a strong near-neighbor electron attractive interaction was identified in one-dimensional (1D) cuprate chains, which may be mediated by phonons [31,32]. Such an interaction is likely to also be a missing ingredient in high- $T_c$  cuprates. Intuitively, the extended Hubbard model (EHM) with on-site repulsion and near-neighbor electron attraction may favor nonlocal Cooper pairs [33,34]. Moreover, a recent DMRG study has identified dominant  $p$ -wave SC correlations in the pairing channel in the one-dimensional (1D) EHM [35]. These recent experimental and theoretical discoveries motivate the investigation of  $d$ -wave superconductivity with the presence of a near-neighbor attractive electron interaction.

*Principal results.* Previous DMRG studies [21–23] have shown that the ground state of the lightly doped Hubbard model on four-leg square cylinders with next-nearest-neighbor (NNN) electron hopping  $t'$  is consistent with that of a Luther-Emery (LE) liquid [36], which is characterized by quasi-long-range SC and charge-density-wave (CDW) correlations but exponentially decaying spin-spin and single-particle correlations. However, while both the CDW and SC correlations are quasi-long range, the former dominates over the latter in all cases, which suggests that CDW order may be realized in two dimensions. In this Letter, we show that the presence of a finite nearest-neighbor (NN) electron attraction  $V$  can notably enhance the SC correlations, while suppressing the CDW correlations simultaneously. This demonstrates the

\*hcjiang@stanford.edu

mutual competition relation between the SC and CDW orders in the Hubbard model. More importantly, we find that the SC correlations become dominant over the CDW correlations when the electron attraction is modestly strong. Our results provide a promising pathway to potentially realize long-range superconductivity in the Hubbard model.

*Model and method.* We use the DMRG method [37] to study the ground-state properties of the single-band extended Hubbard model on the square lattice, defined by the Hamiltonian

$$H = - \sum_{ij,\sigma} t_{ij} (\hat{c}_{i\sigma}^\dagger \hat{c}_{j\sigma} + \text{H.c.}) + U \sum_i \hat{n}_{i\uparrow} \hat{n}_{i\downarrow} + V \sum_{(ij)} \hat{n}_i \hat{n}_j. \quad (1)$$

Here,  $\hat{c}_{i\sigma}^\dagger$  ( $\hat{c}_{i\sigma}$ ) is the electron creation (annihilation) operator with spin- $\sigma$  ( $\sigma = \uparrow, \downarrow$ ) on site  $i = (x_i, y_i)$ , and  $\hat{n}_{i\sigma} = \hat{c}_{i\sigma}^\dagger \hat{c}_{i\sigma}$  and  $\hat{n}_i = \sum_{\sigma} \hat{n}_{i\sigma}$  are the electron number operators. The electron hopping amplitude  $t_{ij}$  equals  $t$  when  $i$  and  $j$  are the nearest neighbors, and equals  $t'$  for next-nearest neighbors.  $U$  is the on-site repulsive Coulomb interaction.  $V$  is the NN electron interaction, where  $V < 0$  and  $V > 0$  represent electron attraction and repulsion, respectively. We take the lattice geometry to be cylindrical with a lattice spacing of unity. The boundary condition of the cylinders is periodic along the  $\hat{y} = (0, 1)$  direction and open in the  $\hat{x} = (1, 0)$  direction. Here, we focus on four-leg cylinders where the width is  $L_y = 4$  and length up to  $L_x = 64$ , with  $L_x$  and  $L_y$  the number of lattice sites along the  $\hat{x}$  and  $\hat{y}$  directions, respectively. The doped hole concentration is defined as  $\delta = N_h/N$ , where  $N = L_y \times L_x$  is the total number of lattice sites and  $N_h$  is the number of doped holes. For the present study, we consider the lightly doped case with hole-doping concentration  $\delta = 12.5\%$ . We set  $t = 1$  as an energy unit, and focus on  $U = 12$  and  $t' = -0.25$  as a representative parameter set. In our calculations, we keep up to  $m = 16\,000$  number of states in each DMRG block with a typical truncation error  $\epsilon \sim 10^{-6}$ . We provide more numerical details in the Supplemental Material [38].

*Charge-density-wave order.* To describe the charge density properties of the ground state of the system, we have calculated the charge density profile  $n(x, y) = \langle \hat{n}(x, y) \rangle$  and its local rung average  $n(x) = \sum_{y=1}^{L_y} n(x, y)/L_y$ . For relatively weak electron attraction  $V$ , e.g.,  $V = -0.1$  as shown in the inset of Fig. 1, the charge density distribution  $n(x)$  is consistent with the ‘‘half-filled’’ charge stripe [21,25,39,40] of wavelength  $\lambda_c = \frac{1}{2\delta}$ , i.e., spacings between two adjacent stripes, with half a doped hole per unit cell. This is consistent with previous DMRG studies of the single-band Hubbard model in the absence of electron attraction, i.e.,  $V = 0$  [21–23]. Accordingly, the ordering wave vector  $Q = 2\pi/\lambda_c$  can be obtained by fitting the charge density oscillation induced by the boundaries of the cylinder [41,42],

$$n(x) \approx \frac{A \cos(Qx + \phi_1)}{[L_{\text{eff}} \sin(\pi x/L_{\text{eff}} + \phi_2)]^{K_c/2}} + n_0. \quad (2)$$

Here,  $A$  is a nonuniversal amplitude,  $\phi_1$  and  $\phi_2$  are the phase shifts,  $K_c$  is the Luttinger exponent, and  $n_0$  is the mean density. We find that an effective length of  $L_{\text{eff}} \sim L_x - 2$  best describes our results. As expected, we find that  $\lambda_c \sim 4$  ( $Q = 4\pi\delta \sim \pi/2$ ) for the half-filled charge stripe.

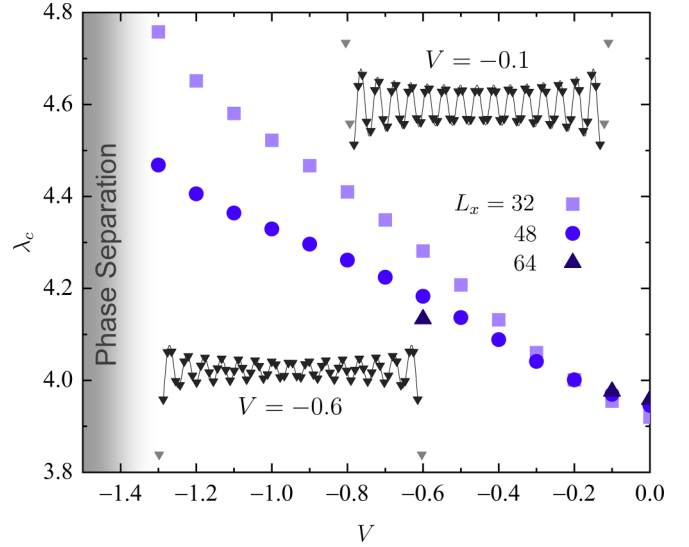


FIG. 1. The CDW wavelength  $\lambda_c$  as a function of  $V$ . The length of the cylinder is  $L_x = 32, 48$ , and  $64$ , and the hole-doping concentration is  $1/8$ . Inset: Charge density profiles for  $V = -0.1$  and  $-0.6$ , respectively. The fitting curves are obtained using Eq. (2). Note that a few data points close to the boundaries (in gray) are removed in the fittings to minimize boundary effects. The gray shaded area denotes phase separation.

When the electron attraction becomes relatively strong, the CDW wavelength  $\lambda_c$  starts deviating notably from the half-filled charge stripes on a finite cylinder (see Fig. 1 insets). We note that such a deviation for both  $\lambda_c$  and  $Q$  from their half-filled stripe values becomes smaller with the increase of the length of the cylinders, suggesting that this deviation could be a finite-size effect. This is indeed supported by the finite-size scaling of  $Q$ , as shown in Fig. 2(b). It is clear that in the long cylinder limit, i.e.,  $L_x \rightarrow \infty$  or  $1/L_x \rightarrow 0$ ,  $Q$  for all different  $V$  will converge to the same value  $Q = 4\pi\delta = \pi/2$ , where  $\lambda_c = 1/2\delta = 4$  at  $\delta = 12.5\%$ . As a result, the half-filled charge stripes may restore in the thermodynamic limit. It is also interesting to note that for cuprates such as  $\text{La}_{2-x}\text{Ba}_x\text{CuO}_4$  (LBCO) and  $\text{La}_{2-x}\text{Sr}_x\text{CuO}_4$  (LSCO) near 12.5% hole doping, the CDW wave vector  $Q$  determined from scattering measurements is always smaller than that expected for the half-filled charge stripe of  $4\pi\delta$  [43–46]. Consider

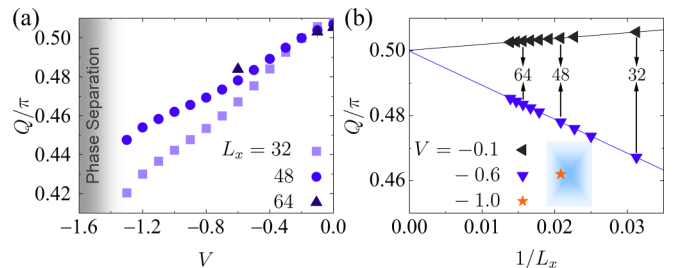


FIG. 2. (a) The CDW ordering wave vector  $Q$  as a function of electron attraction  $V$  and (b) the inverse of the cylinder length  $L_x$  for different  $V$ . The blue shaded area labels the CDW wave vector  $Q = (0.462 \pm 0.01)\pi$  and charge stripe correlation length  $\xi_{\text{cc}} = (10.5 \pm 1.5)\lambda_c$  for  $\text{La}_{2-x}\text{Ba}_x\text{CuO}_4$  with  $x = 0.125$  [43].

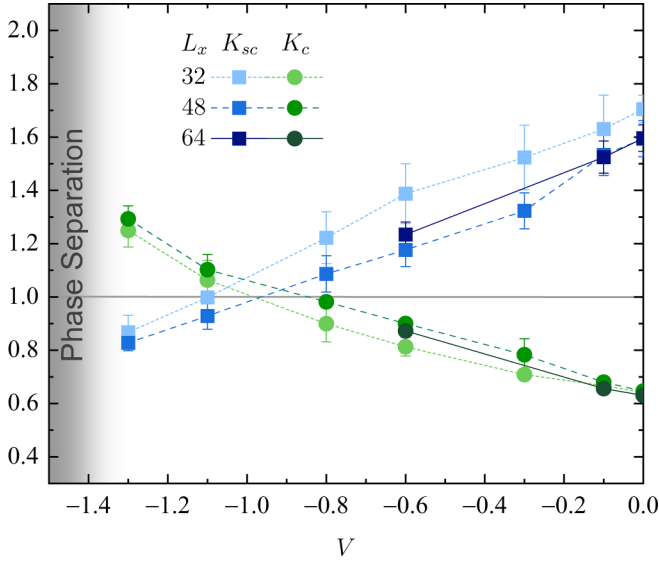


FIG. 3. The extracted Luttinger exponents  $K_{sc}$  and  $K_c$  as a function of the strength of electron attraction  $V$  on different cylinders of length  $L_x$ . The grey shaded area denotes phase separation.

the fact that experimentally the charge order in cuprates is short range with a correlation length of  $\xi_{co} \approx 11\lambda_c$  in LBCO [43] and  $\xi_{co} \approx 3\lambda_c$  in LSCO [44–46]. Our results, shown in Fig. 2(b), on finite-length cylinders (with  $L_x$  comparable to  $\xi_{co}$  in cuprates) are suggestive of significant electron attraction  $V$  in these materials, where the estimated values of electron attraction (in the context of the single-band Hubbard model) are  $V \approx -1.0(2)$  in LBCO and  $V \approx -0.40(5)$  in LSCO.

Importantly, another prominent observation in our study is that while half-filled charge stripes may be restored in the thermodynamic limit, their amplitude and strength are monotonically suppressed by the electron attraction. This is supported by the fact that the CDW exponent  $K_c$  defined in Eq. (2) notably increases with the increase of electron attraction  $|V|$ , as shown in Fig. 3. For instance, we find that  $K_c = 0.65(1)$  for  $V = -0.1$ , while  $K_c = 0.87(1)$  for  $V = -0.6$  on the four-leg cylinder of length  $L_x = 64$ , with an apparent insensitivity to the length of the ladders used in this study. It is worth mentioning that when  $V \lesssim -1.0$ , the CDW order is sufficiently suppressed to be secondary, where the SC correlation becomes dominant, as shown in Fig. 3.

*Superconducting correlation.* To describe the superconducting properties of the ground state of the system, we have calculated the equal-time spin-singlet SC correlation function,

$$\Phi_{\alpha\beta}(r, y) = \langle \Delta_{\alpha}^{\dagger}(x_0, y_0) \Delta_{\beta}(x_0 + r, y_0 + y) \rangle. \quad (3)$$

Here,  $\Delta_{\alpha}^{\dagger}(x, y) = \frac{1}{\sqrt{2}} [\hat{c}_{(x,y),\uparrow}^{\dagger} \hat{c}_{(x,y)+\alpha,\downarrow}^{\dagger} - \hat{c}_{(x,y),\downarrow}^{\dagger} \hat{c}_{(x,y)+\alpha,\uparrow}^{\dagger}]$  is spin-singlet pair creation operator on the bond  $\alpha = \hat{x}$  or  $\hat{y}$ .  $(x_0, y_0)$  is the reference bond with  $x_0 \sim L_x/4$ ,  $r$  is the distance between two bonds in the  $\hat{x}$  direction, and  $y$  is the displacement between two bonds in the  $\hat{y}$  direction. We have calculated different components of the SC correlation, including  $\Phi_{xx}$ ,  $\Phi_{xy}$ , and  $\Phi_{yy}$ , and find that the pairing symmetry is consistent with the plaquette  $d$ -wave symmetry [23,24]. This is characterized by  $|\Phi_{yy}(r, 0)| \gg |\Phi_{xy}(r, 0)| \gg |\Phi_{xx}(r, 0)|$  and  $\Phi_{yy}(r, 0) = -\Phi_{yy}(r, 1)$ .

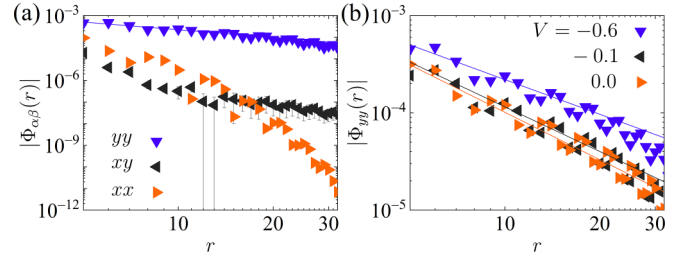


FIG. 4. (a) The superconducting pair-field correlation function for  $V = -0.6$  and (b) charge density profile for  $V = -0.6, -0.1$ , and  $0.0$ . The cylinder length is  $L_x = 64$  and the solid lines are a power-law fitting using  $\Phi_{yy}(r) \sim r^{-K_{sc}}$ .

Similar to the CDW correlation, at long distances,  $\Phi_{yy}(r)$  is characterized by a power law, as shown in Fig. 4(a), with the appropriate Luttinger exponent  $K_{sc}$  defined by

$$\Phi_{yy}(r) \sim r^{-K_{sc}}. \quad (4)$$

As mentioned, previous studies [21–23] of four-leg square cylinders have shown that without electron attraction, that is,  $V = 0$ , the CDW correlations dominate over the SC correlations as  $K_c < K_{sc}$ . It is hence highly nontrivial to find a way to enhance the SC correlations while suppressing the CDW order.

In the previous section, we have shown that CDW correlations can be notably suppressed by NN electron attraction  $V$ . Accordingly, we would expect that the SC correlations can be enhanced by the NN electron attraction  $V$  since the CDW and SC orders are mutually competing [47]. Our numerical results are indeed consistent with this expectation. As shown in Fig. 3, SC correlations become dominant over CDW correlations when  $V \lesssim -1.0$ , where  $K_{sc} < K_c$ . While a slow decay of SC correlations with  $K_{sc} < 2$  implies a SC susceptibility that diverges as  $\chi \sim T^{-(2-K_{sc})}$  as the temperature  $T \rightarrow 0$ , a much smaller  $K_{sc}$ , i.e.,  $K_{sc} \sim 1$ , would lead to a much more divergent SC susceptibility. It is worth mentioning that while adding a near-neighbor attraction flips the dominant order, the ground state of the system is still consistent with that of a LE liquid phase where  $K_{sc}K_c \sim 1$ .

*Spin-spin and single-particle correlations.* To describe the magnetic properties of the ground state, we calculate the spin-spin correlation function defined as

$$F(r) = \langle \vec{S}_{x_0, y_0} \cdot \vec{S}_{x_0 + r, y_0} \rangle. \quad (5)$$

Here,  $\vec{S}_{x,y}$  is the spin operator on site  $i = (x, y)$  and  $i_0 = (x_0, y_0)$  is the reference site with  $x_0 \sim L_x/4$ . Figure 5(a) shows  $F(r)$  for a four-leg cylinder of length  $L_x = 64$ . It is clear that  $F(r)$  decays exponentially as  $F(r) \sim e^{-r/\xi_s}$  at long distances, with a finite correlation length  $\xi_s$ . This is consistent with a finite excitation gap in the spin sector. Moreover, we find that  $\xi_s$  decreases with increasing  $|V|$ , e.g.,  $\xi_s = 7.8(1)$  for  $V = -0.1$  and  $\xi_s = 7.0(2)$  for  $V = -0.6$ . This suppression of short-range antiferromagnetic correlations may thus help to destabilize CDW order and promote SC order. Consistent with previous studies [21–23],  $F(r)$  displays spatial modulations with wavelengths twice that of the charge.

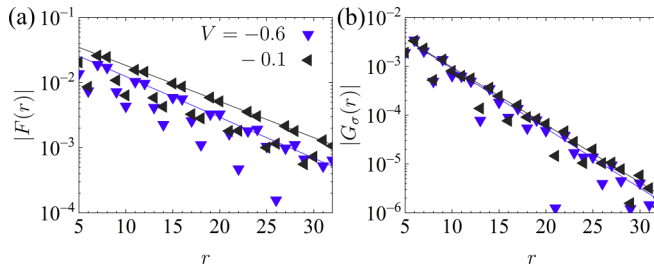


FIG. 5. (a) The spin-spin and (b) single-particle correlation functions with electron attraction  $V = -0.6$  and  $V = -0.1$ . The length of the cylinder is  $L_x = 64$ . Solid lines denote exponential fit  $F(r) \sim e^{-r/\xi_s}$  and  $G_\sigma(r) \sim e^{-r/\xi_G}$ , where  $\xi_s$  and  $\xi_G$  are the corresponding correlation lengths.

We have also calculated the single-particle Green's function, defined as

$$G_\sigma(r) = \langle c_{x_0, y_0, \sigma}^\dagger c_{x_0+r, y_0, \sigma} \rangle. \quad (6)$$

Examples of  $G_\sigma(r)$  are shown in Fig. 5(b). The long-distance behavior of  $G_\sigma(r)$  is consistent with exponential decay  $G_\sigma(r) \sim e^{-r/\xi_G}$ . Similar to  $\xi_s$ , we find that  $\xi_G$  also decreases with the increase of  $|V|$ . For instance, the extracted correlation lengths are  $\xi_G = 3.7(1)$  for  $V = -0.1$  and  $\xi_G = 3.5(1)$  for  $V = -0.6$ , respectively. These are consistent with that of the LE phase.

*Summary and discussion.* In this Letter, we have studied the ground-state properties of the lightly doped extended Hubbard model on the four-leg square cylinders in the presence of near-neighbor electron attraction. Taken together, our results show that the ground state of the system is consistent with a LE liquid [36] where both CDW and SC correlations decay as a power law and  $K_{sc}K_c \sim 1$ . However, previous studies [21–23] show that SC correlations are secondary when  $V = 0$  compared with CDW correlations since  $K_c < 1 < K_{sc}$ . Interestingly, we find that the near-neighbor electron attraction  $V$  can notably enhance SC correlations while simultaneously suppressing CDW correlations. As a result, when  $V \lesssim -1.0$ , SC correlations become dominant while CDW correlations become secondary as  $K_{sc} < 1 < K_c$ . Note that this is a numerical realization of dominant superconductivity in doping the *uniform* Hubbard model on the square lattice of width that is wider than a two-leg ladder. While in this Letter we have

focused on the effect of electron attraction  $V$  on the LE liquid phase on four-leg cylinders, it will also be interesting to study its effect on doping a qualitatively distinct phase such as the insulating “filled” stripe phases [48–50] with  $t' = 0$ , as well as on wider six- and eight-leg square cylinders, to see whether a superconducting phase can be likewise obtained when  $V$  is sufficiently strong. Answering these questions may lead to a better understanding of the mechanism of high-temperature superconductivity.

We note that the critical  $V_c$ , where superconductivity starts to dominate in our simulation, is consistent with the recently identified attractive interaction in 1D cuprates  $\text{Ba}_{2-x}\text{Sr}_x\text{CuO}_{3+\delta}$  [31]. Considering the chemical similarity, it is reasonable to believe that the effective near-neighbor attraction in the  $\text{CuO}_2$  plane is comparable to  $V \sim -t$ . Therefore, our finding suggests the importance of additional interactions beyond the Hubbard model to stabilize superconductivity over CDW. Future high-resolution experiments, such as photoemission and x-ray scattering, and their comparisons with numerical simulations may quantify this effective interaction  $V$  in high- $T_c$  cuprates, in a similar way as for the 1D cuprate chains.

Another approach to estimate this effective  $V$  in realistic materials is a microscopic analysis of the cuprates' crystal and electronic structure. Site phonons coupled with electronic density are possible candidates to mediate such an attractive interaction, which has been quantitatively discussed [32,51]. However, the combined impact of other phonons and other bosonic excitations may contribute to this effective interaction and ultimately result in the strong  $d$ -wave superconductivity in cuprates.

We would like to thank Steven Kivelson for insightful discussions. This work was supported by the U.S. Department of Energy, Office of Science, Basic Energy Sciences, Materials Sciences and Engineering Division, under Contract No. DE-AC02-76SF00515. Parts of the computing for this project were performed at the National Energy Research Scientific Computing Center (NERSC), a U.S. Department of Energy Office of Science User Facility operated under Contract No. DE-AC02-05CH11231. Parts of the computing for this project were performed on the Sherlock cluster. Y.W. acknowledges support from the National Science Foundation (NSF) Award No. DMR-2132338.

- [1] J. G. Bednorz and K. A. Müller, Possible high- $T_c$  superconductivity in the Ba-La-Cu-O system, *Z. Phys. B* **64**, 189 (1986).
- [2] D. J. Scalapino, E. Loh Jr, and J. E. Hirsch,  $d$ -wave pairing near a spin-density-wave instability, *Phys. Rev. B* **34**, 8190 (1986).
- [3] C. Gros, R. Joynt, and T. M. Rice, Superconducting instability in the large- $U$  limit of the two-dimensional Hubbard model, *Z. Phys. B Condens. Matter* **68**, 425 (1987).
- [4] G. Kotliar and J. Liu, Superexchange mechanism and  $d$ -wave superconductivity, *Phys. Rev. B* **38**, 5142 (1988).

- [5] C. C. Tsuei and J. R. Kirtley, Pairing symmetry in cuprate superconductors, *Rev. Mod. Phys.* **72**, 969 (2000).
- [6] F. C. Zhang and T. M. Rice, Effective Hamiltonian for the superconducting Cu oxides, *Phys. Rev. B* **37**, 3759 (1988).
- [7] Editorial, The Hubbard model at half a century, *Nat. Phys.* **9**, 523 (2013).
- [8] B. Keimer, S. A. Kivelson, M. R. Norman, S. Uchida, and J. Zaanen, From quantum matter to high-temperature superconductivity in copper oxides, *Nature (London)* **518**, 179 (2015).

- [9] D. P. Arovas, E. Berg, S. A. Kivelson, and S. Raghu, The Hubbard model, *Annu. Rev. Condens. Matter Phys.* **13**, 239 (2022).
- [10] M. Qin, T. Schäfer, S. Andergassen, P. Corboz, and E. Gull, The Hubbard model: A computational perspective, *Annu. Rev. Condens. Matter Phys.* **13**, 275 (2022).
- [11] P. W. Anderson, The Resonating Valence Bond State in  $\text{La}_2\text{CuO}_4$  and superconductivity, *Science* **235**, 1196 (1987).
- [12] E. Dagotto, Correlated electrons in high-temperature superconductors, *Rev. Mod. Phys.* **66**, 763 (1994).
- [13] B.-X. Zheng, C.-M. Chung, P. Corboz, G. Ehlers, M.-P. Qin, R. M. Noack, H. Shi, S. R. White, S. Zhang, and G. K.-L. Chan, Stripe order in the underdoped region of the two-dimensional Hubbard model, *Science* **358**, 1155 (2017).
- [14] E. W. Huang, C. B. Mendl, Shenxiu Liu, S. Johnston, H.-C. Jiang, B. Moritz, and T. P. Devereaux, Numerical evidence of fluctuating stripes in the normal state of high- $T_c$  cuprate superconductors, *Science* **358**, 1161 (2017).
- [15] E. W. Huang, C. B. Mendl, H.-C. Jiang, B. Moritz, and T. P. Devereaux, Stripe order from the perspective of the Hubbard model, *npj Quantum Mater.* **3**, 22 (2018).
- [16] B. Ponsioen, S. S. Chung, and P. Corboz, Period 4 stripe in the extended two-dimensional Hubbard model, *Phys. Rev. B* **100**, 195141 (2019).
- [17] J. Kokalj, Bad-metallic behavior of doped Mott insulators, *Phys. Rev. B* **95**, 041110(R) (2017).
- [18] E. W. Huang, R. Sheppard, B. Moritz, and T. P. Devereaux, Strange metallicity in the doped Hubbard model, *Science* **366**, 987 (2019).
- [19] P. Cha, A. A. Patel, E. Gull, and E.-A. Kim, Slope invariant T-linear resistivity from local self-energy, *Phys. Rev. Res.* **2**, 033434 (2020).
- [20] M. Qin, C.-M. Chung, H. Shi, E. Vitali, C. Hubig, U. Schollwöck, S. R. White, and S. Zhang, Absence of Superconductivity in the Pure Two-Dimensional Hubbard Model, *Phys. Rev. X* **10**, 031016 (2020).
- [21] H.-C. Jiang and T. P. Devereaux, Superconductivity in the doped Hubbard model and its interplay with next-nearest hopping  $t'$ , *Science* **365**, 1424 (2019).
- [22] Y.-F. Jiang, J. Zaanen, T. P. Devereaux, and H.-C. Jiang, Ground state phase diagram of the doped Hubbard model on the four-leg cylinder, *Phys. Rev. Res.* **2**, 033073 (2020).
- [23] C.-M. Chung, M. Qin, S. Zhang, U. Schollwöck, and S. R. White, Plaquette versus ordinary  $d$ -wave pairing in the  $t'$ -Hubbard model on a width-4 cylinder, *Phys. Rev. B* **102**, 041106(R) (2020).
- [24] J. F. Dodaro, H.-C. Jiang, and S. A. Kivelson, Intertwined order in a frustrated four-leg  $t$ - $J$  cylinder, *Phys. Rev. B* **95**, 155116 (2017).
- [25] H.-C. Jiang, Z.-Y. Weng, and S. A. Kivelson, Superconductivity in the doped  $t$ - $J$  model: Results for four-leg cylinders, *Phys. Rev. B* **98**, 140505(R) (2018).
- [26] S. Jiang, D. J. Scalapino, and S. R. White, Ground State Phase Diagram of the  $t$ - $t'$ - $J$  Model, *Proc. Natl. Acad. Sci. USA* **118**, e2109978118 (2021).
- [27] H.-C. Jiang and S. A. Kivelson, High Temperature Superconductivity in a Lightly Doped Quantum Spin Liquid, *Phys. Rev. Lett.* **127**, 097002 (2021).
- [28] S. Gong, W. Zhu, and D. N. Sheng, Robust  $d$ -Wave Superconductivity in the Square-Lattice  $t$ - $J$  model, *Phys. Rev. Lett.* **127**, 097003 (2021).
- [29] H.-C. Jiang, S. Chen, and Z.-Y. Weng, Critical role of the sign structure in the doped Mott insulator: Luther-Emery versus Fermi-liquid-like state in quasi-one-dimensional ladders, *Phys. Rev. B* **102**, 104512 (2020).
- [30] H.-C. Jiang and S. A. Kivelson, Stripe order enhanced superconductivity in the Hubbard model, *Proc. Natl. Acad. Sci.* **119**, e2109406119 (2022).
- [31] Z. Chen, Y. Wang, S. N. Rebec, T. Jia, M. Hashimoto, D. Lu, B. Moritz, R. G. Moore, T. P. Devereaux, and Z.-X. Shen, Anomalous strong near-neighbor attraction in doped 1d cuprate chains, *Science* **373**, 1235 (2021).
- [32] Y. Wang, Z. Chen, T. Shi, B. Moritz, Z.-X. Shen, and T. P. Devereaux, Phonon-Mediated Long-Range Attractive Interaction in One-Dimensional Cuprates, *Phys. Rev. Lett.* **127**, 197003 (2021).
- [33] M. Jiang, Enhancing  $d$ -wave superconductivity with nearest-neighbor attraction in the extended Hubbard model, *Phys. Rev. B* **105**, 024510 (2022).
- [34] Z.-B. Huang, S.-C. Fang, and H.-Q. Lin, Superconductivity, nematicity, and charge density wave in high- $T_c$  cuprates: A common thread, [arXiv:2109.05519](https://arxiv.org/abs/2109.05519).
- [35] D.-W. Qu, B.-B. Chen, H.-C. Jiang, Y. Wang, and W. Li, Spin-triplet pairing induced by near-neighbor attraction in the extended Hubbard model for cuprate chain, *Commun. Phys.* **5**, 257 (2022).
- [36] A. Luther and V. J. Emery, Backward Scattering in the One-Dimensional Electron Gas, *Phys. Rev. Lett.* **33**, 589 (1974).
- [37] S. R. White, Density Matrix Formulation for Quantum Renormalization Groups, *Phys. Rev. Lett.* **69**, 2863 (1992).
- [38] See Supplemental Material at <http://link.aps.org/supplemental/10.1103/PhysRevB.107.L201102> for further numerical details, including finite error extrapolations  $L_x$  and  $U/t$  dependence of the extended Hubbard model.
- [39] S. R. White and D. J. Scalapino, Ground states of the doped four-leg  $t$ - $j$  ladder, *Phys. Rev. B* **55**, R14701 (1997).
- [40] S. R. White and D. J. Scalapino, Competition between stripes and pairing in a  $t - t' - j$  model, *Phys. Rev. B* **60**, R753 (1999).
- [41] S. R. White, I. Affleck, and D. J. Scalapino, Friedel oscillations and charge density waves in chains and ladders, *Phys. Rev. B* **65**, 165122 (2002).
- [42] M. Dolfi, B. Bauer, S. Keller, and M. Troyer, Pair correlations in doped Hubbard ladders, *Phys. Rev. B* **92**, 195139 (2015).
- [43] M. Hücker, M. V. Zimmermann, G. D. Gu, Z. J. Xu, J. S. Wen, G. Xu, H. J. Kang, A. Zheludev, and J. M. Tranquada, Stripe order in superconducting  $\text{La}_{2-x}\text{Ba}_x\text{CuO}_4$  ( $0.095 \leq x \leq 0.155$ ), *Phys. Rev. B* **83**, 104506 (2011).
- [44] V. Thampy, M. P. M. Dean, N. B. Christensen, L. Steinke, Z. Islam, M. Oda, M. Ido, N. Momono, S. B. Wilkins, and J. P. Hill, Rotated stripe order and its competition with superconductivity in  $\text{La}_{1.88}\text{Sr}_{0.12}\text{CuO}_4$ , *Phys. Rev. B* **90**, 100510(R) (2014).
- [45] T. P. Croft, C. Lester, M. S. Senn, A. Bombardi, and S. M. Hayden, Charge density wave fluctuations in  $\text{La}_{2-x}\text{Sr}_x\text{CuO}_4$  and their competition with superconductivity, *Phys. Rev. B* **89**, 224513 (2014).
- [46] J.-J. Wen, H. Huang, S.-J. Lee, H. Jang, J. Knight, Y. S. Lee, M. Fujita, K. M. Suzuki, S. Asano, S. A. Kivelson, C.-C. Kao,

- and J.-S. Lee, Observation of two types of charge-density-wave orders in superconducting  $\text{La}_{2-x}\text{Sr}_x\text{CuO}_4$ , *Nat. Commun.* **10**, 3269 (2019).
- [47] E. Fradkin, S. A. Kivelson, and J. M. Tranquada, Colloquium: Theory of intertwined orders in high temperature superconductors, *Rev. Mod. Phys.* **87**, 457 (2015).
- [48] J. Zaanen and O. Gunnarsson, Charged magnetic domain lines and the magnetism of high- $T_c$  oxides, *Phys. Rev. B* **40**, 7391 (1989).
- [49] K. Machida, Magnetism in  $\text{La}_2\text{CuO}_4$  based compounds, *Physica C: Superconductivity* **158**, 192 (1989).
- [50] M. Kato, K. Machida, H. Nakanishi, and M. Fujita, Soliton lattice modulation of incommensurate spin density wave in two dimensional Hubbard model -A mean field study-, *J. Phys. Soc. Jpn.* **59**, 1047 (1990).
- [51] S. Karakuzu, A. Tanjaroon Ly, P. Mai, J. Neuhaus, T. A. Maier, and S. Johnston, Stripe correlations in the two-dimensional Hubbard-Holstein model, *Commun. Phys.* **5**, 311 (2022).